Electronic Supplementary Material (ESI) for Inorganic Chemistry Frontiers.

Supporting Information for

"Zinc-dependent switching mechanism from an open to a new closed-state conformation of insulin-degrading enzyme"

Karina Abramov-Harpaz[1,2] Yifat Miller[1,2,*]

[1]*Department of Chemistry, Ben-Gurion University of the Negev, P.O. Box 653, Be'er Sheva 84105, Israel*

[2] *Ilse Katz Institute for Nanoscale Science and Technology, Ben-Gurion University of the Negev, Beér-Sheva 84105, Israel*

Corresponding author:

*Yifat Miller: ymiller@bgu.ac.il

Table of Contents

Methods and Materials

Construction of two IDE structural models

The initial structure of the of insulin-degrading enzyme (IDE) that was applied in this work is based on an experimental structure that was solved by cryo-EM, and that was solved in the dimeric form that is complexed with an insulin monomer (PDB ID code: 6BF8).[1] The monomer with the largest open-state conformation between IDE-N and IDE-C was isolated from the dimer and was used to construct two different structural models of the IDE. It is important to note that this experimental IDE structure lacks the Zn^{2+} ion in the catalytic zinc-containing binding site. Thus, one structural model was taken as is, in absence of Zn^{+2} ion at the active site, and in the second structural model Zn^{2+} ion was inserted into the catalytic zinc-containing binding site. The modeling procedure was performed by using the Accelrys Discovery Studio software package.[2] Constrain distances between the Zn^{2+} ion and the atoms of the side chains of residues H108, H112, E189 have been applied to conserve the active binding site.

Molecular Dynamics (MD) simulations protocol

The MD simulations of the solvated constructed models were performed in the NPT ensemble using NAMD package[3] with the CHARMM27 forcefield with the CMAP correlation.[4] The energies of each cyclosporine phospholipid-enzyme were minimized and the model explicitly solvated in a TIP3P water box.[5, 6] Each water molecule within 2.5 Å of the models was removed. Counter ions were added at random locations to neutralize the models' charge. The Langevin piston method[3, 7, 8] with a decay period of 100 fs and a damping time of 50 fs was used to maintain a constant pressure of 1 atm. The temperature 330K was controlled by a Langevin thermostat with a damping coefficient of 10 ps.[3] The short-range van der Waals (VDW) interactions were calculated using the switching function, with a twin range cutoff of 10.0 and 12.0 Å. Long-range electrostatic interactions were calculated using the particle mesh Ewald method with a cutoff of 12.0 Å.[9, 10] The equations of motion were integrated using the leapfrog integrator with a step of 1 fs. The counter ions and water molecules were allowed to move. The hydrogen atoms were constrained to the equilibrium bond using the SHAKE algorithm.[11] The minimized solvated systems were energy minimized for 5000 additional conjugate gradient steps and 20,000 heating steps at 250 K, with all

atoms allowed to move. Then, the system was heated from 250 K to 300 K and then to 330 K for 300 ps and equilibrated at 330 K for 300 ps. The choice of the higher temperature than physiological temperature is to investigate the stability of the constructed models. Obviously, structures that are stable at higher temperature, will be also stable at physiological temperature. Simulations ran for 200 ns for each variant model. The structures were saved every 10 ps for analyses.

To ensure the production of the new closed-state IDE conformation, three further trajectories of MD simulations were performed for a different initial conformation IDE (Figure S4a). The velocities were differing between the three trajectories. In the first trajectory the equilibrate temperature was at 310 K. In the second trajectory it was at 280 K and in the third trajectory it was 250 K. The MD simulation was ended until the new closed state IDE conformation was observed. Our simulations showed that the new closed state IDE conformation was observed for all three trajectories after 30 ns (Figure S4b, S4c, and S4d).

Structural analyses

The structural stabilities of the two models were measured by using several analyses. The convergence of domains within IDE and the partition of closed and open states of IDE in both models were analyzed by the root-mean-square-deviation (RMSD) analysis. The fluctuations evaluation was conducted for each residue within IDE via root-mean-square-fluctuation (RMSF) analysis. To determine the secondary structure of the IDE, the database of secondary structure of protein (DSSP) method[12] has been applied for the first 5 ns of the simulations to the open-state conformation and for the last 5 ns of the simulations for the closed-state conformation of IDE in presence of Zn^{2+} ion in the catalytic zinc-containing binding site. For the IDE in absence of Zn^{2+} ion in the catalytic zinc-containing binding site, the DSSP was calculated for the partially open-state conformation and the full open-state conformation that were observed along the MD simulations. This method was applied to provide the percentage of the α-helix or β-strand for each residue within the IDE along the MD simulations. Examination of necessary interactions and motions within IDE were performed by measuring the distance between residues within IDE.

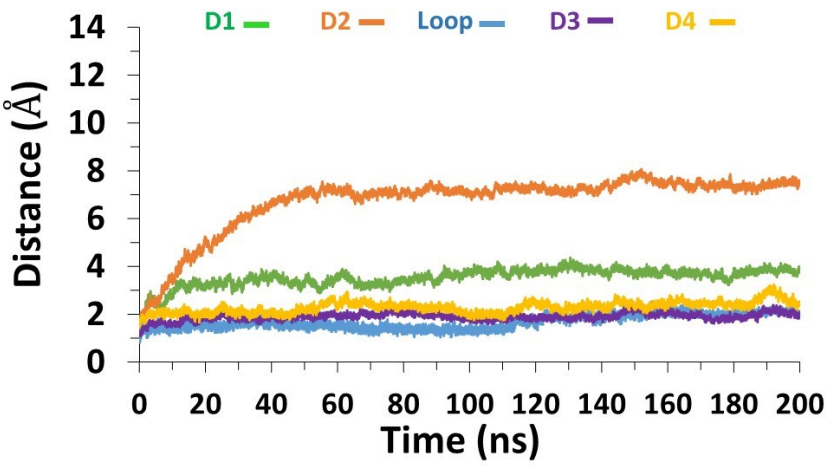

Figure S1: The Root Mean Square Deviation (RMSD) values of IDE along the MD simulations demonstrates convergence of the IDE structure which is in presence of Zn^{2+} at the catalytic zinc-containing binding site.

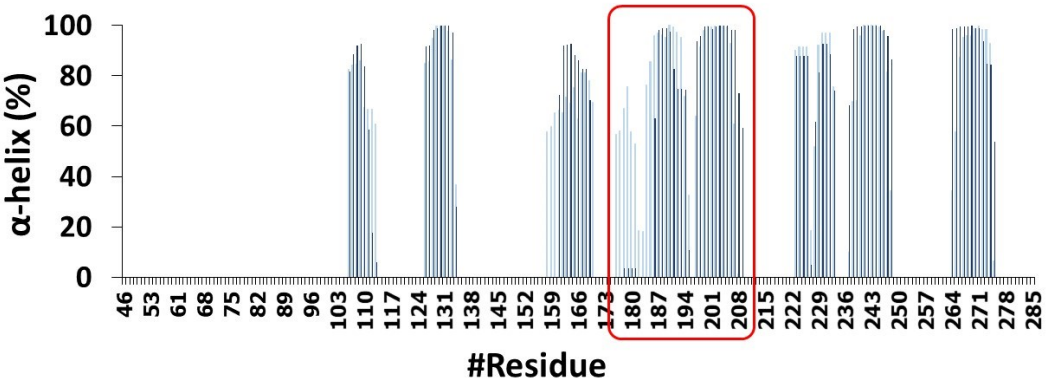

Figure S2: The percentages of α-helix along the sequence of domain D1 of IDE for the open-state IDE conformation (color: light blue) and for the closed-state IDE conformation (color: blue). The door subdomain sequence is marked in the red rectangle.

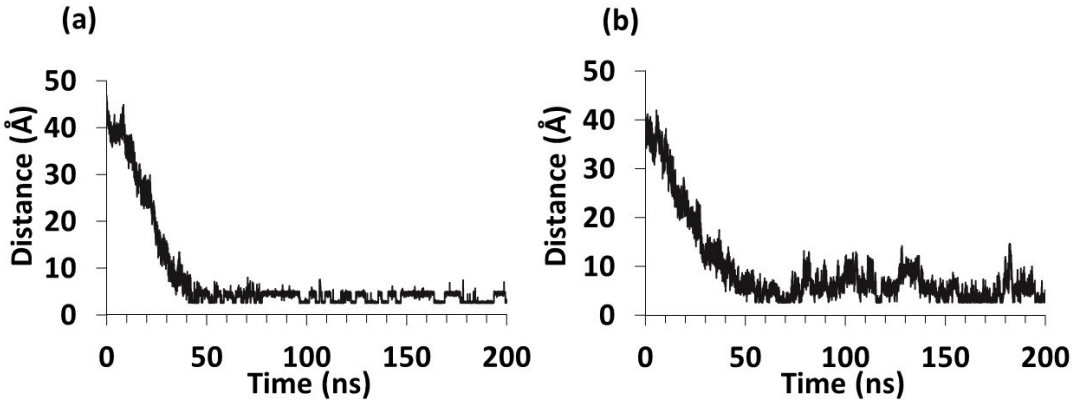

Figure S3: (a) The distance between Cα atom of residue E191 in domain D1 and Cα atom of residue K657 in domain D4 along the MD simulations; (b) The distance between Cα atom of residue K192 in domain D1 and Cα atom of residue E664 in domain D4 along the MD simulations.

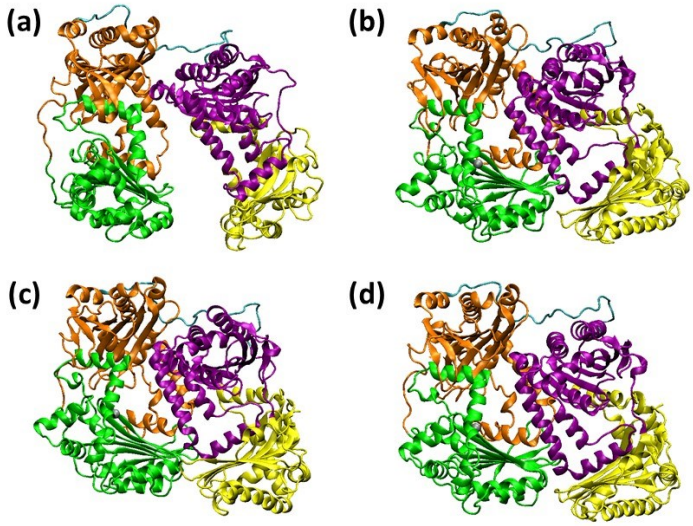

Figure S4: (a) Initial minimized structure of IDE in presence of Zn^{2+} derived (taken from 30 ns of the original MD simulations). This structure was used for further three trajectories of MD simulations. (b) Simulated structure of the first trajectory at 250K, observed after 30 ns. (c) Simulated structure of the first trajectory at 280K, observed after 30 ns. (d) Simulated structure of the first trajectory at 310 K, observed after 30 ns. Domain D1 (color: green), domain D2 (color: orange), domain D3 (color: purple), domain D4 (color: yellow).

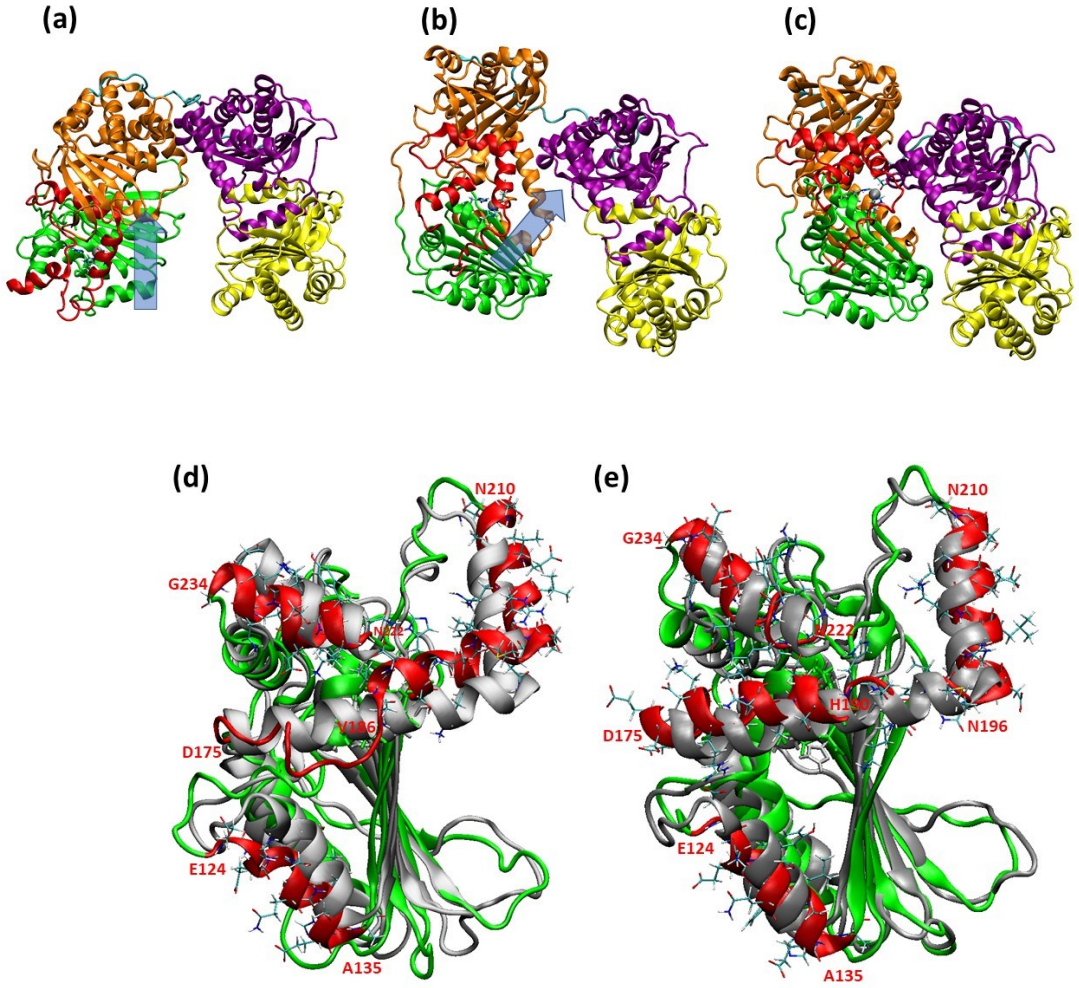

Figure S5: The structure of IDE in presence of Zn^{2+} at the catalytic zinc-containing binding site at (a) 1 ns, (b) 30 ns, and (c) 200 ns of the MD simulations: A shift between the IDE-N and the IDE-C domain occurs (a) and then Domain D1 (color: green) incoming to domain D3 (color: purple) (b); Superimpose structure of domain D1 (residues 46-285) of initial IDE structure (color: gray) and final simulated IDE structure in IDE structure (color: red) which is (d) in presence of Zn^{2+} and (e) in absence of Zn^{2+} at the catalytic zinc-containing binding site. Only the helices that are shown here in colors red and gray are those that show the shift change along the MD simulations. While in absence of Zn^{2+} the door subdomain does not swing and change, in presence of Zn^{2+} the door subdomain is swinging, due to the movement to form electrostatic interactions between domain D1 and domain D3.

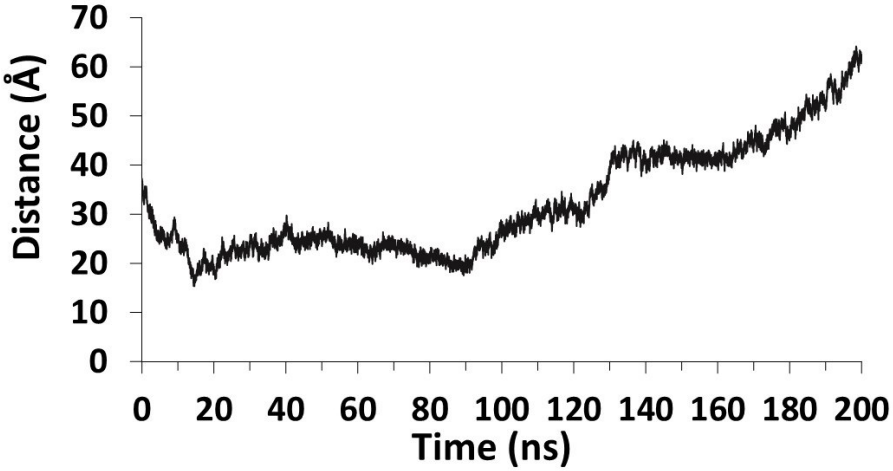

Figure S6: The distance between Cα atom of residue E133 in domain D1 and Cα atom of residue E880 in domain D4 along the MD simulations.

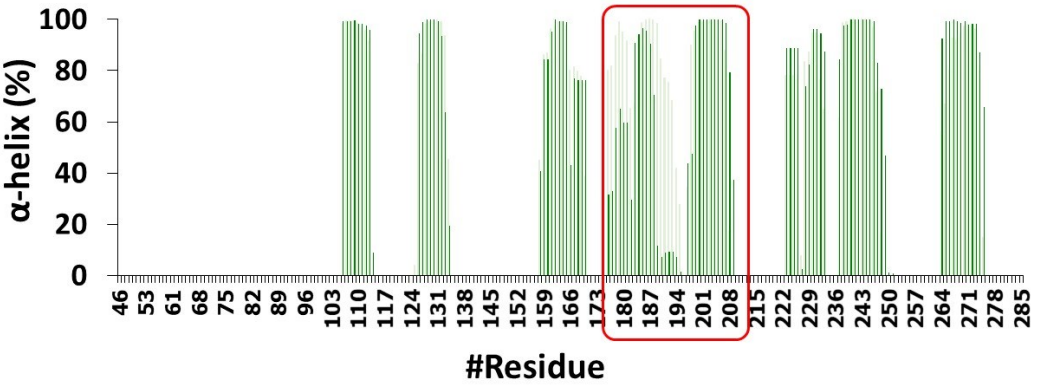

Figure S7: The percentages of α-helix along the sequence of domain D1 of IDE for the partially open-state IDE conformation (color: light green) and for the fully open-state IDE conformation (color: green). The door subdomain sequence is marked in the red rectangle.

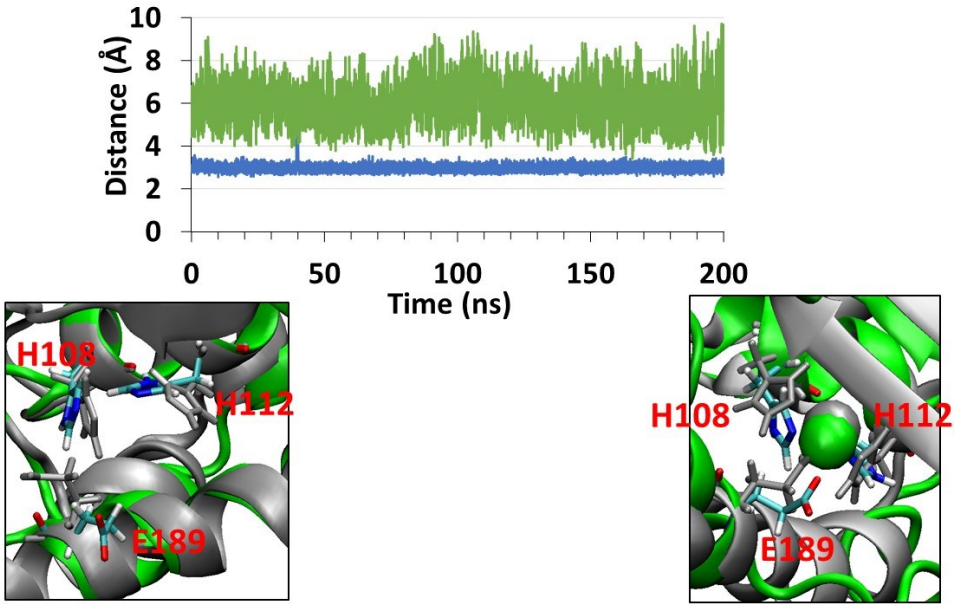

Figure S8: The distance between atom Nε of residue H112 and the carboxylic O atom of E189 in IDE in absence of Zn^{2+} (color: green), and in presence of Zn^{2+} at the catalytic zinc-containing binding site (color: blue) along the MD simulations. Superimpose of initial minimized IDE structure at the catalytic zinc-containing binding site (residues H108, H112, E189) (color: gray) and the final simulated IDE structure at the catalytic zinc-containing binding site (color: green) for IDE in absence of Zn^{2+} (left), and in presence of Zn^{2+} at the catalytic zinc-containing binding site (right).

Table S1: The averaged distances and the standard deviation in Å, between the Zn^{2+} ion and the residues that bind the ion for the open-state conformation and the close-state conformation of IDE. The measured values for the open-state conformation were taken from 5-30 ns of the simulations, and for the close-state conformation were taken from 50-200 ns.

	Open-state conformation	Close-state conformation
Zn^{2+}- Nε (His108)	2.23 ± 0.07	2.22 ± 0.07
Zn^{2+}- Nε (His112)	2.21 ± 0.07	2.23 ± 0.07
Zn^{2+}- O carboxylic atom (Glu189)	1.99 ± 0.06	1.98 ± 0.05

References

1. Zhang Z, Liang WG, Bailey LJ, et al. Ensemble cryoEM elucidates the mechanism of insulin capture and degradation by human insulin degrading enzyme. *Elife*. 2018;7. doi:10.7554/eLife.33572.
2. http://accelrys.com/products/discovery-studio/
3. Kalé, L.; Skeel, R.; Bhandarkar, M.; Brunner, R.; Gursoy, A.; Krawetz, N.; Phillips, J.; Shinozaki, A.; Varadarajan, K.; Schulten, K., NAMD2: Greater Scalability for Parallel Molecular Dynamics. *Journal of Computational Physics* 1999, 151, 283-312.
4. MacKerell, A. D.; Bashford, D.; Bellott, M.; Dunbrack, R. L.; Evanseck, J. D.; Field, M. J.; Fischer, S.; Gao, J.; Guo, H.; Ha, S.; Joseph-McCarthy, D.; Kuchnir, L.; Kuczera, K.; Lau, F. T.; Mattos, C.; Michnick, S.; Ngo, T.; Nguyen, D. T.; Prodhom, B.; Reiher, W. E.; Roux, B.; Schlenkrich, M.; Smith, J. C.; Stote, R.; Straub, J.; Watanabe, M.; Wiorkiewicz-Kuczera, J.; Yin, D.; Karplus, M., All-atom empirical potential for molecular modeling and dynamics studies of proteins. *The journal of physical chemistry. B* 1998, 102, 3586-616.
5. Jorgensen, W. L.; Chandrasekhar, J.; Madura, J. D.; Impey, R. W.; Klein, M. L., Comparison of simple potential functions for simulating liquid water. *The Journal of chemical physics* 1983, 79, 926-935.
6. Mahoney, M. W.; Jorgensen, W. L., A five-site model for liquid water and the reproduction of the density anomaly by rigid, nonpolarizable potential functions. *J Chem Phys* 2000, 112, 8910-8922.
7. Feller, S. E.; Zhang, Y.; Pastor, R. W.; Brooks, B. R., Constant pressure molecular dynamics simulation: the Langevin piston method. *The Journal of chemical physics* 1995, 103, 4613-4621.
8. Tu, K.; Tobias, D. J.; Klein, M. L., Constant pressure and temperature molecular dynamics simulation of a fully hydrated liquid crystal phase dipalmitoylphosphatidylcholine bilayer. *Biophysical journal* 1995, 69, 2558.
9. Darden, T.; York, D.; Pedersen, L., Particle mesh Ewald: An N· log (N) method for Ewald sums in large systems. *The Journal of chemical physics* 1993, 98, 10089-10092.

10. Essmann, U.; Perera, L.; Berkowitz, M. L.; Darden, T.; Lee, H.; Pedersen, L. G., A smooth particle mesh Ewald method. *The Journal of chemical physics* 1995, 103, 8577-8593.
11. Ryckaert, J.-P.; Ciccotti, G.; Berendsen, H. J., Numerical integration of the cartesian equations of motion of a system with constraints: molecular dynamics of n-alkanes. *Journal of Computational Physics* 1977, 23, 327-341.
12. Kabsch, W.; Sander, C., Dictionary of protein secondary structure: pattern recognition of hydrogen-bonded and geometrical features. *Biopolymers* 1983, 22, 2577-637.